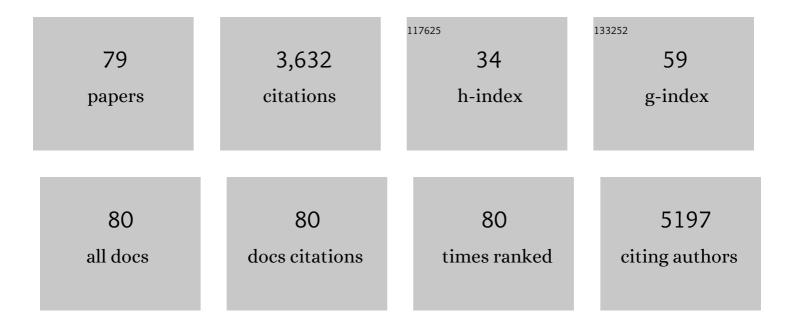
## Philippe Moreau

List of Publications by Year in descending order

Source: https://exaly.com/author-pdf/3205090/publications.pdf Version: 2024-02-01



#	Article	IF	CITATIONS
1	Structure and Stability of Sodium Intercalated Phases in Olivine FePO <sub>4</sub> . Chemistry of Materials, 2010, 22, 4126-4128.	6.7	436
2	The failure mechanism of nano-sized Si-based negative electrodes for lithium ion batteries. Journal of Materials Chemistry, 2011, 21, 6201.	6.7	317
3	A low-cost and high performance ball-milled Si-based negative electrode for high-energy Li-ion batteries. Energy and Environmental Science, 2013, 6, 2145.	30.8	274
4	Enhanced and tunable surface plasmons in two-dimensional <mml:math xmlns:mml="http://www.w3.org/1998/Math/MathML"&gt;<mml:mrow><mml:msub><mml:mi>Ti</mml:mi><mml:m mathvariant="normal"&gt;C<mml:mn>2</mml:mn></mml:m </mml:msub></mml:mrow>stacks: Electronic structure versus boundary effects. Physical Review B, 2014, 89, .</mml:math 	n>33.2	l:mn>122
5	Multiprobe Study of the Solid Electrolyte Interphase on Silicon-Based Electrodes in Full-Cell Configuration. Chemistry of Materials, 2016, 28, 2557-2572.	6.7	116
6	Is LiFePO[sub 4] Stable in Water?. Electrochemical and Solid-State Letters, 2008, 11, A4.	2.2	98
7	Relativistic effects in electron-energy-loss-spectroscopy observations of theSi/SiO2interface plasmon peak. Physical Review B, 1997, 56, 6774-6781.	3.2	97
8	Reversible anion intercalation in a layered aromatic amine: a high-voltage host structure for organic batteries. Journal of Materials Chemistry A, 2016, 4, 6131-6139.	10.3	97
9	New insights into the silicon-based electrode's irreversibility along cycle life through simple gravimetric method. Journal of Power Sources, 2012, 220, 180-184.	7.8	93
10	Critical Role of Silicon Nanoparticles Surface on Lithium Cell Electrochemical Performance Analyzed by FTIR, Raman, EELS, XPS, NMR, and BDS Spectroscopies. Journal of Physical Chemistry C, 2014, 118, 17318-17331.	3.1	89
11	SulfurK-Edge X-Ray-Absorption Study of the Charge Transfer upon Lithium Intercalation into Titanium Disulfide. Physical Review Letters, 1996, 77, 2101-2104.	7.8	88
12	Strong anisotropic influence of local-field effects on the dielectric response of <mml:math xmlns:mml="http://www.w3.org/1998/Math/MathML" display="inline"&gt;<mml:mi>î±</mml:mi>-MoO<mml:math xmlns:mml="http://www.w3.org/1998/Math/MathML" display="inline"&gt;<mml:msub><mml:mrow< td=""><td>3.2</td><td>88</td></mml:mrow<></mml:msub></mml:math </mml:math 	3.2	88
13	/> <mml:mn>3</mml:mn> . Physical Review B, 2013, 88, . An electrochemically roughened Cu current collector for Si-based electrode in Li-ion batteries. Journal of Power Sources, 2013, 239, 308-314.	7.8	78
14	Evidence of a rutile-phase characteristic peak in low-energy loss spectra. Physical Review B, 2004, 69, .	3.2	77
15	Elucidation of the Na <sub>2/3</sub> FePO <sub>4</sub> and Li <sub>2/3</sub> FePO <sub>4</sub> Intermediate Superstructure Revealing a Pseudouniform Ordering in 2D. Journal of the American Chemical Society, 2014, 136, 9144-9157.	13.7	67
16	Mechanism of Silicon Electrode Aging upon Cycling in Full Lithiumâ€Ion Batteries. ChemSusChem, 2016, 9, 841-848.	6.8	67
17	Very High Surface Capacity Observed Using Si Negative Electrodes Embedded in Copper Foam as 3D Current Collectors. Advanced Energy Materials, 2014, 4, 1301718.	19.5	64
18	Quantitative use of electron energy-loss spectroscopy Mo-M2,3 edges for the study of molybdenum oxides. Ultramicroscopy, 2015, 149, 1-8.	1.9	60

PHILIPPE MOREAU

#	Article	IF	CITATIONS
19	Correlation between irreversible capacity and electrolyte solvents degradation probed by NMR in Si-based negative electrode of Li-ion cell. Electrochemistry Communications, 2013, 33, 72-75.	4.7	59
20	Hierarchical and Resilient Conductive Network of Bridged Carbon Nanotubes and Nanofibers for High-Energy Si Negative Electrodes. Electrochemical and Solid-State Letters, 2009, 12, A76.	2.2	55
21	Stability of LiFePO4 in water and consequence on the Li battery behaviour. Ionics, 2008, 14, 583-587.	2.4	49
22	Nanoscale Chemical Evolution of Silicon Negative Electrodes Characterized by Low-Loss STEM-EELS. Nano Letters, 2016, 16, 7381-7388.	9.1	45
23	Electron energy-loss spectra calculations and experiments as a tool for the identification of a lamellarC3N4compound. Physical Review B, 2006, 73, .	3.2	41
24	Quantitative MAS NMR characterization of the LiMn1/2Ni1/2O2 electrode/electrolyte interphase. Solid State Nuclear Magnetic Resonance, 2012, 42, 51-61.	2.3	41
25	Dual Anion–Cation Reversible Insertion in a Bipyridinium–Diamide Triad as the Negative Electrode for Aqueous Batteries. Advanced Energy Materials, 2018, 8, 1701988.	19.5	41
26	Experimental and theoretical studies of the electronic structure of TiS2. Physical Review B, 1996, 54, R11009-R11013.	3.2	40
27	Interpretation of preedge features in the Ti and S K-edge x-ray-absorption near-edge spectrain the layered disulfidesTiS2andTaS2. Physical Review B, 1997, 55, 9508-9513.	3.2	40
28	Origin of valence and core excitations in LiFePO <sub>4</sub> and FePO <sub>4</sub> . Journal of Physics Condensed Matter, 2010, 22, 275501.	1.8	40
29	Thermomechanical Polymer Binder Reactivity with Positive Active Materials for Li Metal Polymer and Li-Ion Batteries: An XPS and XPS Imaging Study. ACS Applied Materials & Interfaces, 2019, 11, 18368-18376.	8.0	40
30	Effect of glutaric anhydride additive on the LiNi0.4Mn1.6O4 electrode/electrolyte interface evolution: A MAS NMR and TEM/EELS study. Journal of Power Sources, 2012, 215, 170-178.	7.8	39
31	Synthesis of nanosized Si particles via a mechanochemical solid–liquid reaction and application in Li-ion batteries. Solid State Ionics, 2007, 178, 1297-1303.	2.7	38
32	Abnormal operando structural behavior of sodium battery material: Influence of dynamic on phase diagram of NaxFePO4. Electrochemistry Communications, 2014, 38, 104-106.	4.7	38
33	Electronic structures and charge transfer in lithium and mercury intercalated titanium disulfides. Journal of Physics and Chemistry of Solids, 1996, 57, 1117-1122.	4.0	36
34	Valence electron energy-loss spectroscopy of silicon negative electrodes for lithium batteries. Physical Chemistry Chemical Physics, 2010, 12, 220-226.	2.8	36
35	Fast determination of phases in LixFePO4 using low losses in electron energy-loss spectroscopy. Applied Physics Letters, 2009, 94, .	3.3	35
36	From Si wafers to cheap and efficient Si electrodes for Li-ion batteries. Journal of Power Sources, 2014, 256, 32-36.	7.8	34

PHILIPPE MOREAU

#	Article	IF	CITATIONS
37	Ab initiosimulation of the electron energy-loss near-edge structures at the LiKedge in Li,Li2O, andLiMn2O4. Physical Review B, 2006, 74, .	3.2	33
38	Structural Investigation of Mercury-Intercalated Titanium Disulfide. 1. The Crystal Structure of Hg1.24TiS2. Chemistry of Materials, 1995, 7, 1132-1139.	6.7	29
39	Improved comparison of low energy loss spectra with band structure calculations: the example of BN filaments. Ultramicroscopy, 2003, 94, 293-303.	1.9	28
40	Synergistic Effect in Carbon Coated LiFePO <sub>4</sub> for High Yield Spontaneous Grafting of Diazonium Salt. Structural Examination at the Grain Agglomerate Scale. Journal of the American Chemical Society, 2013, 135, 11614-11622.	13.7	25
41	Nanoscale compositional changes during first delithiation of Si negative electrodes. Journal of Power Sources, 2013, 227, 237-242.	7.8	25
42	Coaxial nickel/poly(p-phenylene vinylene) nanowires as luminescent building blocks manipulated magnetically. Nanotechnology, 2009, 20, 405601.	2.6	23
43	First evidence of resistive switching in polycrystalline GaV <sub>4</sub> S <sub>8</sub> thin layers. Physica Status Solidi - Rapid Research Letters, 2011, 5, 53-55.	2.4	23
44	Degradation diagnosis of aged Li4Ti5O12/LiFePO4 batteries. Journal of Power Sources, 2014, 267, 744-752.	7.8	21
45	Structural Investigation of Mercury-Intercalated Titanium Disulfide. 2. HRTEM of HgxTiS2. Chemistry of Materials, 1995, 7, 1140-1152.	6.7	20
46	Formation of Li[sub 1+n]V[sub 3]O[sub 8]â^β-Li[sub 1â^•3]V[sub 2]O[sub 5]â^•C Nanocomposites by Carboreduction and the Resulting Improvement in Li Capacity Retention. Journal of the Electrochemical Society, 2006, 153, A295.	2.9	20
47	Revisiting lithium K and iron M2,3 edge superimposition: The case of lithium battery material LiFePO4. Micron, 2012, 43, 16-21.	2.2	20
48	Determination of Lithium Insertion Sites in LixTiP4(x= 2â^'11) by Electron Energy-Loss Spectroscopy. Journal of Physical Chemistry C, 2007, 111, 3996-4002.	3.1	19
49	Electrical characterizations of resistive random access memory devices based on GaV4S8 thin layers. Thin Solid Films, 2013, 533, 61-65.	1.8	19
50	Toward the Aqueous Processing of Li <sub>4</sub> Ti <sub>5</sub> O <sub>12</sub> : A Comparative Study with LiFePO <sub>4</sub> . Journal of the Electrochemical Society, 2012, 159, A1083-A1090.	2.9	17
51	XPS and SEM-EDX Study of Electrolyte Nature Effect on Li Electrode in Lithium Metal Batteries. ACS Applied Energy Materials, 0, , .	5.1	17
52	Carbonate and Ionic Liquid Mixes as Electrolytes To Modify Interphases and Improve Cell Safety in Silicon-Based Li-Ion Batteries. Chemistry of Materials, 2017, 29, 8132-8146.	6.7	15
53	Local field effects at Li K edges in electron energy-loss spectra of Li,Li2Oand LiF. Physical Review B, 2008, 77, .	3.2	14
54	Electric field induced avalanche breakdown and non-volatile resistive switching in the Mott Insulators AM4Q8. European Physical Journal: Special Topics, 2013, 222, 1046-1056.	2.6	14

Philippe Moreau

#	Article	IF	CITATIONS
55	NMR quantitative analysis of solid electrolyte interphase on aged Li-ion battery electrodes. Electrochimica Acta, 2015, 155, 391-395.	5.2	14
56	NMR monitoring of electrode/electrolyte interphase in the case of air-exposed and carbon coated LiFePO 4. Journal of Power Sources, 2013, 243, 682-690.	7.8	13
57	Peculiar Li-storage mechanism at graphene edges in turbostratic carbon black and their application in high energy Li-ion capacitor. Journal of Power Sources, 2018, 378, 628-635.	7.8	13
58	Study of Li1+xV3O8 by band structure calculations and spectroscopies. Journal of Physics and Chemistry of Solids, 2006, 67, 1238-1242.	4.0	11
59	Redirected charge transport arising from diazonium grafting of carbon coated LiFePO <sub>4</sub> . Physical Chemistry Chemical Physics, 2014, 16, 22745-22753.	2.8	11
60	Engineered Electronic Contacts for Composite Electrodes in Li Batteries Using Thiophene-Based Molecular Junctions. Chemistry of Materials, 2015, 27, 4057-4065.	6.7	11
61	From the Direct Observation of a PAAâ€Based Binder Using STEMâ€VEELS to the Ageing Mechanism of Silicon/Graphite Anode with High Areal Capacity Cycled in an FECâ€Rich and ECâ€Free Electrolyte. Advanced Energy Materials, 2022, 12, 2103348.	19.5	11
62	Electronic structure of a hole doped oxide with a quasi-1D crystal structure Y2â^'x(Sr,Ca)xBaNiO5. Journal of Alloys and Compounds, 2001, 317-318, 149-152.	5.5	9
63	Deposition by radio frequency magnetron sputtering of GaV4S8 thin films for resistive random access memory application. Thin Solid Films, 2013, 533, 54-60.	1.8	9
64	Mercury sublattice melting transition in the misfit intercalation compound H1.24TiS2. Journal of Physics and Chemistry of Solids, 1996, 57, 1129-1132.	4.0	8
65	Electron energy-loss spectroscopy in the low-loss region as a characterization tool of electrode materials. Ionics, 2008, 14, 191-195.	2.4	8
66	Formation of Li1+nV3O8/β-Li1/3V2O5/C nanocomposites by carboreduction and resulting improvements of the capacity retention. Journal of Physics and Chemistry of Solids, 2006, 67, 1312-1314.	4.0	7
67	Mercury Intercalation into Lamellar Transition Metal Disulfides. Molecular Crystals and Liquid Crystals, 1994, 244, 325-330.	0.3	6
68	Structural and physical properties of the misfit intercalation compoundsHgxTaS2(x=0.58, 1.19, and 1.3). Physical Review B, 1995, 52, 11359-11371.	3.2	6
69	Fabrication and performance of electrochemically grafted thiophene silicon nanoparticle anodes for Li-ion batteries. Journal of Power Sources, 2016, 324, 97-105.	7.8	6
70	A hybrid method using the widely-used WIEN2k and VASP codes to calculate the complete set of XAS/EELS edges in a hundred-atoms system. Physical Chemistry Chemical Physics, 2017, 19, 1320-1327.	2.8	6
71	Energy loss spectroscopic profiling across linear interfaces: The example of amorphous carbon superlattices. Ultramicroscopy, 2006, 106, 346-355.	1.9	5
72	Nanoconfined nonequilibrium electrodeposition of metal-metal hydroxide one-dimensional nanostructures. Electrochimica Acta, 2015, 151, 347-354.	5.2	5

PHILIPPE MOREAU

#	Article	IF	CITATIONS
73	TEM Study of the Misfit Intercalation Compounds .alphaHg1.19TaS2 and .betaHg1.3TaS2. Inorganic Chemistry, 1995, 34, 5496-5500.	4.0	3
74	Electron energy loss spectroscopy analysis of lithium deintercalated Li5/3â^'xTi7/3CrO7. Journal of Physics and Chemistry of Solids, 2006, 67, 1295-1298.	4.0	3
75	Subnanometer-resolved measurement of the tunneling effective mass using bulk plasmons. Applied Physics Letters, 2006, 88, 122109.	3.3	3
76	New airtight transfer box for SEM experiments: Application to lithium and sodium metals observation and analyses. Micron, 2018, 110, 10-17.	2.2	3
77	Mercury Intercalation in Titanium and Tantalum Disulfides. NATO ASI Series Series B: Physics, 1993, , 351-354.	0.2	2
78	Application of a Cryo-FIB-SEM-μRaman Instrument to Probe the Depth of Vitreous Ice in a Frozen Sample. Analytical Chemistry, 2022, 94, 8120-8125.	6.5	2
79	XANES Study of the Charge Transfer upon Lithium Intercalation into Lamellar Transition Metal Dichalcogenides. European Physical Journal Special Topics, 1997, 7, C2-257-C2-258.	0.2	0